AGU PUBLICATIONS

JGR

Journal of Geophysical Research: Space Physics

RESEARCH ARTICLE
10.1002/2015JA021815

Key Points:
- Spatial electron precipitation structures can persist for over a minute
- Spatial structures can be only a few tens of kilometers wide
- Closely spaced satellites can separate temporal from spatial structure

Correspondence to:
J. B. Blake,
JBernard.Blake@aero.org

Citation:
Blake, J. B., and T. P. O'Brien (2016), Observations of small-scale latitudinal structure in energetic electron precipitation, *J. Geophys. Res. Space Physics*, *121*, 3031–3035, doi:10.1002/2015JA021815.

Received 18 AUG 2015
Accepted 4 MAR 2016
Accepted article online 9 MAR 2016
Published online 9 APR 2016

Observations of small-scale latitudinal structure in energetic electron precipitation

J. B. Blake[1] and T. P. O'Brien[1]

[1]Space Science Applications Laboratory, The Aerospace Corporation, Los Angeles, California, USA

Abstract We describe first-light observations from the AC6 mission, a pair of CubeSats that are in polar orbit and whose in-track separations range up to several hundred kilometers and whose separations are controlled by differential drag. We present temporal dose rate profiles from electrons greater than 35 keV that are very similar at the two vehicles, but offset in time by the GPS-derived in-track separation. We interpret these structures as spatial and propose that they are the result of multiple microbursts that have experienced bounce phase mixing and differential drift over a small fraction of a drift orbit before reaching the spacecraft.

1. Introduction

Microbursts were observed early in the space science era [*Anderson and Enemark*, 1960; *Brown*, 1961; *Anger et al.*, 1963; *Anderson and Milton*, 1964; *Brown et al.*, 1965; *Oliven et al.*, 1968; *Rosenberg et al.*, 1971; *Imhof et al.*, 1986]. The instrumentation used in much of the early work used balloons carrying X-ray instrumentation. This approach remains a powerful technique and is still in effective use, cf., the Balloon Array for Radiation-belt Relativistic Electron Losses investigation operating in concert with the two Van Allen Probe satellites [*Millan et al.*, 2013]. In the case of the balloon or ground-based measurements a very large area is being viewed, perhaps a circular spot a hundred kilometers or more in diameter. High time measurements are made and bursty structure seen, but it is an integral over a large area in both latitude and longitude. Furthermore, the balloon or ground-based observations can only see the effects of electrons that strike the upper atmosphere above the observing point, which is electrons scattered into the bounce loss cone. Drift-loss cone electrons will pass overhead unseen.

The launch of Solar Anomalous and Magnetospheric Particle Explorer (SAMPEX) gave a major boost to this area of investigation because of the very large geometric factor of the HILT (Heavy Ion Large Telescope) instrument (25 to 100 cm^2 sr) and sampling rates of 10 to 50 times per second [*Klecker et al.*, 1993; *Nakamura et al.*, 1995; *Blake et al.*, 1996; *Nakamura et al.*, 2000; *Lorentzen et al.*, 2001]. The observed microburst precipitation varied markedly on time scales of well under a second, but the problem of separating spatial and temporal variabilities with only a single vantage point remained. This spatiotemporal ambiguity has important implications for quantifying loss rates of radiation belt electrons due to microbursts [e.g., *O'Brien et al.*, 2004; *Saito et al.*, 2012] as well as understanding the underlying physics. The magnitude of the loss rate due to microburst precipitation is important of course for understanding the populations of the radiation belts.

It has been long recognized that two or more spacecraft in close proximity, ideally with time-variable separations, could reveal the scale sizes of precipitation regions and the persistence of fine structure at low altitude. Using observations from the pair of AeroCube6 (AC6) satellites in Polar low Earth orbit (LEO), equipped with energetic particle detectors, we present a case study indicating that fine-scale structures in >35 keV electron microbursts can result from the spatial scale of precipitation events, as well as their temporal duration.

2. Satellites and Instrumentation

The AC6 pair was launched 19 June 2014 aboard a Dnepr launch vehicle. The orbit attained was 620 × 700 km at a 98° inclination. The pair was ejected together and then began to separate in track. Each satellite carries a GPS receiver that gives their locations to ~20 m. The cross-track separation remains at less than 1 km. The pair separated to ~800 km, and then differential drag was used to bring them back closer together. The s/c are

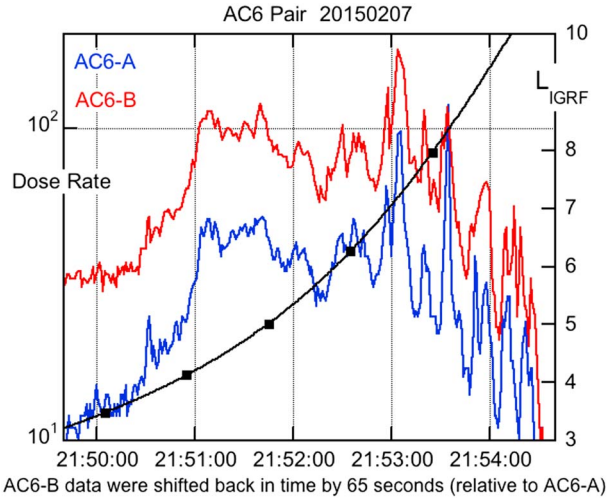

Figure 1. The time history of the dose rate of electrons >35 keV from AC6-A and AC6-B is plotted as a function of time on 7 February 2015, with the AC6-B data shifted back in time by the in-track separation of the two spacecraft (AC6-B trails AC6-A).

Sun pointing, rotating with ~12 s period, thus keeping the solar array normal to the direction to the Sun and maximizing power. The polar orbit of the two s/c means that in-track motion is latitudinal, and therefore, the time history of the measurements is a scan in *L* value.

LEO satellites such as AC6 spend most of the time in the drift loss cone, of the order of 80%. Thus, most of AC6 electron observations are of electrons that will be lost after longitudinal drift brings them to a point where the mirror point drops into the upper atmosphere. Conventionally, this loss altitude is usually taken to be 100 km. The drift time until loss can be minutes to tens of minutes. The location of an AC6 satellite in terms of bounce loss cone, drift loss cone, or stable trapping region is calculated along with many other parameters.

The dosimeters used in this study aboard both CubeSats are nominally identical and are dosimeters that primarily measure the dose in silicon deposited by magnetospheric electrons with energies >35 keV. The dosimeters are sensitive to all radiation that deposits more than 35 keV in the silicon detectors, but magnetospheric energetic particle abundances are such that >35 keV electrons dominate. Electrons with energies from 35 keV to a couple of hundred keV deposit most of the dose because the electron energy spectra, in general, are relatively steep. The two dosimeters were calibrated with a precision charge pulser, however, modest threshold/efficiency differences might well exist that could lead to differences in count rate of a factor of 2 or so in an identical electron environment.

The silicon detectors are 1.8 mm in diameter and 60 μm thick, behind a 1.8 μm aluminum foil. The electronic system measures the energy deposited in this silicon for all deposits greater than 50 keV. Dose is energy deposited per unit mass, so integration of the measured liberated charge is the history of the dose delivered to the silicon. It then follows that the dose rate is readily found by differentiating the dose history. The dose is sampled at 1 s intervals.

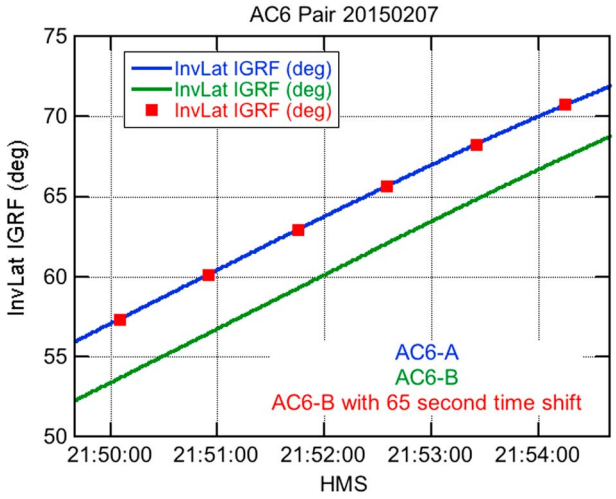

Figure 2. The invariant latitude (InvLat) of the two spacecraft is plotted as a function of time around the time of the observations. In addition, the track for AC6-B is also plotted with the −65 s shift (red squares). This clearly shows the separation of the two spacecraft along their common orbit.

Magnetic torque rods provide all attitude control for the AC6 CubeSats. The spacecraft are Sun pointing and rotate about this axis with a 12 s period. On both spacecraft, the dosimeter is on the antisunward face. A GPS receiver on each spacecraft provides 20 m accuracy on position. Accurate knowledge of the separation of the two AeroCube6 satellites proved to be crucial in discovering the ubiquity of fine spatial structures in the low-altitude energetic electron population.

The ability to control vehicle attitude has enabled the use of differential drag to control the separation of the two spacecraft. After deployment and when first turned on, the separation was 12 km. The

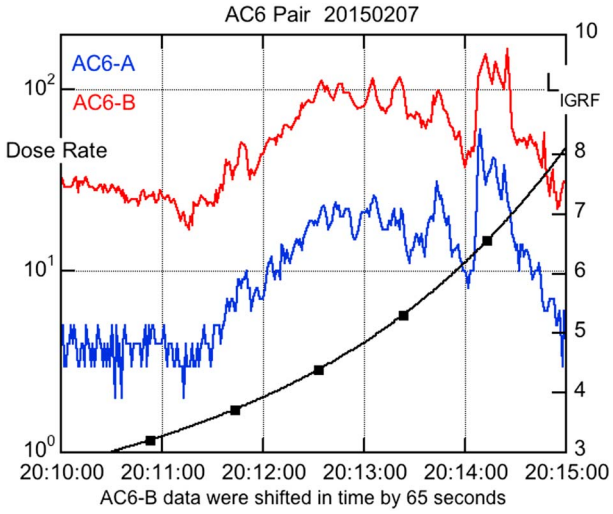

Figure 3. The data from the orbit just prior to that shown in Figure 1 are plotted. Stationary structure in the >35 keV electron precipitation is clearly seen in the data from both vehicles.

separation increased to ~800 km in mid-September 2014 and since has been decreasing. Two time periods are used in this study. The first on 7 February 2015 when the vehicles were separated by ~489 km in-track or about 65 s in time, and the second on 19 May 2015 when the s/c were separated by 46 km in-track or 6.1 s.

3. Observations

A key observation is shown in Figure 1, where the dose rates from the >35 keV dosimeters on both satellites are plotted late in the day on 7 February 2015. A visual comparison of the data from the two spacecraft showed the time histories had very similar structure on both a broad and much finer time scale. Shifting the time scale of AC6-B 65 s forward in time (it is the trailing spacecraft and thus arrives later in a given position along the orbital track) gave a good visual congruence and is so plotted. The GPS-derived position indicates that the in-track separation at that time indeed was 65 s. The persistence of the finer-scale electron intensity structures in the time series of dose rates for over a minute must be due to the persistence of corresponding spatial structures on several scale sizes.

At the time of these observations, the spacecraft pair was passing through the outer radiation belt in the drift loss cone and were passing northeastward over Kamchatka, Russia. Figure 2 shows that the 65 s offset aligns the drift shells [$L = 1/\cos^2(\text{InvLat})$] of the two vehicles, confirming their separation along their common orbit.

Years of SAMPEX microburst observations [e.g., *Lorentzen et al.*, 2001] have shown that microburst precipitation can persist for many hours, and therefore, we might hope to see similar precipitation on adjacent orbits. Figure 3 shows data from the orbit prior to the one giving the data shown in Figure 1. This shows that in a little less than 2 h, the precipitation structures of >35 keV electrons at the same local times have evolved significantly although fine structure remained.

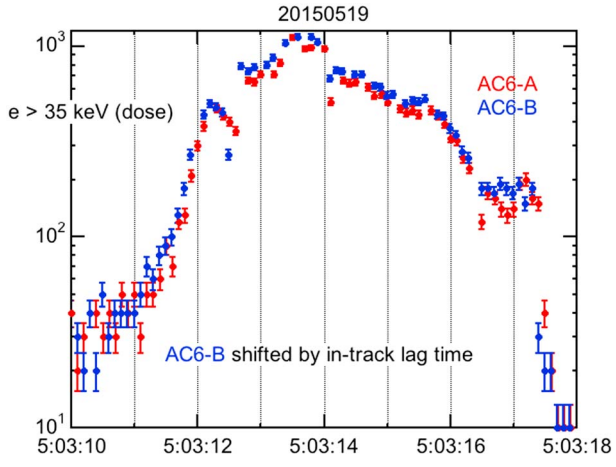

Figure 4. The two CubeSats' dosimeters observe the same temporal details in the precipitating electron population, separated by the 6 s in-track interval. Similar fine details in the time history can be observed in both profiles with good statistics.

In Figure 4, we show another example of quasi-stationary structure in precipitating electrons, this time from 19 May 2015 when the two spacecraft had closed to a separation distance less than 10% of the separation on 7 February 2015.

At times, the two CubeSats encounter broader areas of precipitation where fine structure cannot be discerned, and a broad relatively smooth region of precipitation is seen; Figure 5 is an example of such an observation. Note that the time interval in Figure 5 is several minutes whereas in Figure 4 the time interval is 8 s.

4. Discussion

The width of the precipitation structure in-track can be estimated given that the observations from the two spacecraft

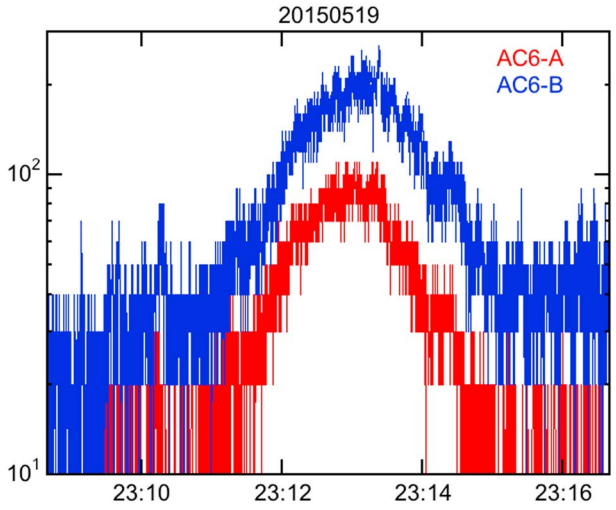

Figure 5. The AC6-A and AC6-B CubeSats encountered a broad region of >35 keV electrons in the drift loss cone. The s/c were in the precipitation region for more than 2 min or over 1000 km in track.

indicate that the structures are actually spatial in origin. At this location in the radiation belts, the drift period for ~50 keV electrons is ~300 min, and the bounce period is about ~1 s for particles mirroring near the loss cone. The 1 s measurement resolution is effectively a bounce average. Conversely, the 65 s separation represents many bounce periods but less than 1% of a drift period or about 60 km of drift motion. The implied longitude extent of the features observed in Figures 1 and 3 is at least ~60 km. To obtain the latitudinal scale size, a narrow structure was selected from the observations, and the time within the structure gave the width given the known orbital velocity of the satellites. Figure 6 shows a feature that is ~4 s wide and thus ~30 km large in the latitude direction.

What might lead to the observed persistent and narrow structures? *Santolik and Gurnett* [2003] found that the perpendicular dimensions of the chorus source region in the equatorial plane were 7–100 km. Such scale sizes, when mapped to low altitude along the magnetic field, would be far smaller than the tens of kilometers for the precipitation features we report. Thus, a single chorus source region that persists for >65 s is not a plausible explanation for the spatial structure.

Suppose, however, that microburst precipitation arising from chorus in several distinct spatial source regions occurred westward of the orbital track of the AC6 pair. The energetic electrons are strongly scattered, some immediately enter the upper atmosphere and others are left in the drift-loss cone. They drift eastward, and now that the strong transient scattering has ended, they remain on the same drift shells. Drift speed depends upon energy so the drifting electrons spread out along the drift path. In this way, a small microburst region will lead to broader (in longitude) curtains of drifting electrons moving eastward that two spacecraft can intercept sequentially. A similar type of structure was seen with SAMPEX in the inner zone due to electron precipitation induced by lightning [*Blake et al.*, 2001]. In the case of this observation there was only a single satellite, SAMPEX. However, complex structures, seen at magnetically conjugate points, made it clear that slowly evolving structures were being observed.

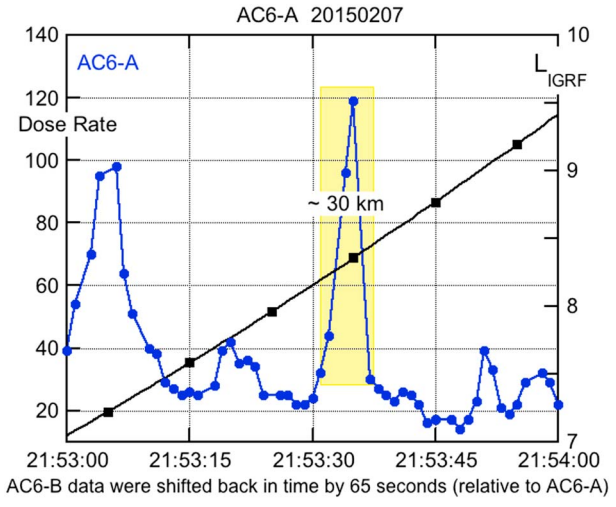

Figure 6. The narrow precipitation feature is ~4 s wide and thus ~ 30 km wide in latitude.

It is crucial to note that complex, fine spatial structures separated by the in-track separation of the two satellites (known to ~ 20 m as noted above) have been observed many dozens of times over the 18 months of the AeroCube6 mission. This coherence is ubiquitous and cannot be due to a chance occurrence of chorus elements.

5. Conclusion

We have presented evidence that low-altitude electron precipitation structures with spatial scale sizes of ~30–60 km persist for at least 65 s for ~35 keV electrons. We measured these structures with dosimeters

aboard a pair of coorbiting CubeSats in Polar LEO. The time and spatial scales are inconsistent with these structures arising from individual chorus elements. However, the scales are consistent with drifting curtains of remnant microburst precipitation. We propose that these curtains mix together multiple microburst events that have mixed together after several bounce periods and have spread out through differential drift over a small fraction of a drift orbit.

Acknowledgments
The authors wish to acknowledge the U.S. Air Force Space and Missile Systems Center Advanced Development Directorate (SMC/AD) for their support of the dosimeter payload and AeroCube6 mission. The authors also would like to acknowledge the many people on the Aerospace AeroCube6 mission engineering team for their superb work that made this research possible. The AeroCube-6 dosimeter data have not yet been approved for public release by the U.S. Air Force at the time of writing. Interest parties may contact the lead author to obtain updated release status.

References

Anderson, K. A., and D. C. Enemark (1960), Balloon observations of X-rays in the auroral zone, high time resolution studies, *J. Geophys. Res.*, *65*, 3521–3538, doi:10.1029/JZ065i011p03521.

Anderson, K. A., and D. W. Milton (1964), Balloon observations of X-rays in the auroral zone II: 3. High time resolution studies, *J. Geophys. Res.*, *69*, 4457–4479, doi:10.1029/JZ069i021p04457.

Anger, C. D., J. R. Barcus, R. R. Brown, and D. S. Evans (1963), Auroral zone X-ray pulsations in the 1 to 15-second range, *J. Geophys. Res.*, *68*, 1023–1030, doi:10.1029/JZ068i004p01023.

Blake, J. B., M. D. Looper, D. N. Baker, R. Nakamura, B. Klecker, and D. Hovestadt (1996), New high temporal and spatial resolution measurements by SAMPEX of the precipitation of relativistic electrons, *Adv. Space Res.*, *18*(8), 171–186.

Blake, J. B., U. S. Inan, M. Walt, T. F. Bell, J. Bortnik, D. L. Chenette, and H. J. Christian (2001), Lightning-induced energetic electron flux enhancements in the drift loss cone, *J. Geophys. Res.*, *106*, 29,733–29,744, doi:10.1029/2001JA000067.

Brown, R. R. (1961), Balloon observations of auroral-zone X-rays, *J. Geophys. Res.*, *66*, 1379–1388, doi:10.1029/JZ066i005p01379.

Brown, R. R., J. R. Barcus, and N. R. Parsons (1965), Balloon observations of auroral zone x rays in conjugate regions: 1. Slow time variations, *J. Geophys. Res.*, *70*, 2579–2598, doi:10.1029/JZ070i011p02579.

Imhof, W. L., H. D. Voss, J. B. Reagan, D. W. Datlowe, E. E. Gaines, J. Mobilia, and D. S. Evans (1986), Relativistic electron and energetic ion precipitation spikes near the plasmapause, *J. Geophys. Res.*, *91*, 3077–3088, doi:10.1029/JA091iA03p03077.

Klecker, B., et al. (1993), HILT: A heavy ion large area proportional counter telescope for solar and anomalous cosmic rays, *IEEE Trans. Geosci. Remote Sens.*, *31*, 542–548.

Lorentzen, K. R., M. D. Looper, and J. B. Blake (2001), Relativistic electron microbursts during the GEM storms, *Geophys. Res. Lett.*, *28*, 2573–2576, doi:10.1029/2001GL012926.

Millan, R. M., et al. (2013), The balloon array for RBSP relativistic electron losses (BARREL), *Space Sci. Rev.*, *179*, 503–530, doi:10.1007/s11214-013-9971-z.

Nakamura, R., D. N. Baker, J. B. Blake, S. Kanekal, B. Klecker, and D. Hovestadt (1995), Relativistic electron precipitation enhancements near the outer edge of the radiation belt, *Geophys. Res. Lett.*, *22*, 1129–1132, doi:10.1029/95GL00378.

Nakamura, R., M. Isowa, Y. Kamide, D. N. Baker, J. B. Blake, and M. Looper (2000), SAMPEX observations of precipitation burst in the outer radiation belt, *J. Geophys. Res.*, *105*, 15,875–15,885, doi:10.1029/2000JA900018.

O'Brien, T. P., M. D. Looper, and J. B. Blake (2004), Quantification of relativistic electron microburst losses during the GEM storms, *Geophys. Res. Lett.*, *31*, L04802, doi:10.1029/2003GL018621.

Oliven, M. N., D. Venkatesan, and K. G. McMacracken (1968), Microburst phenomena: 2. Auroral-zone electrons, *J. Geophys. Res.*, *73*, 2345–2353, doi:10.1029/JA073i007p02345.

Rosenberg, T. J., R. A. Helliwell, and J. P. Katsufrakis (1971), Electron precipitation associated with discrete very-low-frequency emissions, *J. Geophys. Res.*, *76*, 8445–8452, doi:10.1029/JA076i034p08445.

Saito, S., Y. Miyoshi, and K. Seki (2012), Relativistic electron microbursts associated with whistler chorus rising tone elements: GEMSIS-RBW simulations, *J. Geophys. Res.*, *117*, A10206, doi:10.1029/2012JA018020.

Santolik, O., and D. A. Gurnett (2003), Transverse dimensions of chorus in the source region, *Geophys. Res. Lett.*, *30*, 1031, doi:10.1029/2002GL016178.